 NRL Report 4688

DEMON DATA TRANSMISSION LINK-TYPE 2

R.R. Zirm and D.S. Hepler

Avigation and Transistor Research Branch
Electronics Division

February 7, 1956

Naval Research Laboratory
Washington, D.C.

CONTENTS

ABSTRACT

[redacted]

Modifications were made in the DEMON (DElay MOdulated Noise) data transmission link in order to improve its signal-to-noise characteristics and thereby increase the maximum range and security of the system without degrading the expected performance in the presence of propagation noise. A link receiver was developed which has a 13-db improvement in signal-to-noise ratio over that of the original receiver, along with a simplified and more stable decoder. This equipment, with power supply, has been packaged in two standard ATR racks to facilitate flight test. A traveling-wave-tube final amplifier has been used in the transmitter so that a power output of 1.0 watt is obtained.

Theoretical calculations were made to determine the signal-to-noise characteristics of the improved receiver, and they compared favorably with the measured values. A more rigorous analysis of the propagation characteristics of the DEMON data transmission link confirmed the results of previous approximate calculations.

PROBLEM STATUS

This is an interim report on one phase of the problem; work is continuing.

AUTHORIZATION

NRL Problem R04-04
Projects NR 504-420, NL 450-067, NE 010-221,
NE 010-238, and NE 010-221-8
Bureau Nos. S-1536 and EL-9A-368

Manuscript submitted December 22, 1955

DEMON DATA TRANSMISSION LINK - TYPE 2

[CONFIDENTIAL]

INTRODUCTION

In reference 1 certain improvements and modifications were recommended for the DEMON data transmission link, mainly in the configuration of the receiver, to improve the signal-to-noise characteristics of the link and, thereby, its maximum operating range and security. It was further recommended that an effort be made to increase the transmitter power output to a value which would make flight test of the link possible.

Improved receiver operation, along with a reduction in size and weight, was accomplished by employing only one converter stage and one video i-f strip, and by eliminating the multiple frequency local oscillator as recommended in reference 1. This provided a reduction in power supply requirements and in the number of tubes and components, and hence increased the reliability of the equipment. The chief problems in the design of this receiver were overcome by the development of a cascaded stage video i-f amplifier with a flat frequency response from 5 to 100 Mc and an r-f amplifier of 200 Mc bandwidth, and by the design of a more sensitive multiplier.

Very little change was made in the structure of the transmitter, except that a traveling-wave-tube power amplifier* was added to the output.

TRANSMITTER

The basic transmitter was identical to the one described in reference 1, except for the addition of a traveling-wave-tube power amplifier* which increased the average output power from approximately 40 milliwatts to approximately one watt. Slight readjustment of electrode potentials increased the available maximum output power with a minor loss in available gain. Maximum output power for a noise signal was found to be 25 percent less than for a sine wave signal because of the amplitude-limiting effect of the traveling-wave tube. The block diagram of the transmitter is shown in Fig. 1.

RECEIVER THEORY AND PERFORMANCE

Mathematical analysis of the receiver described in reference 1, which used the multiple frequency local oscillator and an r-f delay, indicates that maximum signal-to-noise improvement is not obtainable with that configuration because the bandwidth compression from r-f to i-f is not equivalent to a filtration process. Increasing the i-f bandwidth from 5 Mc to 100 Mc increased the receiver sensitivity by 13 db, i.e.,

$$10 \log \frac{100 \text{ Mc}}{5 \text{ Mc}} = 13\text{-db gain.}$$

*The traveling-wave tube used was a model TWA-L1W manufactured by Roger White Electron Devices, Inc.

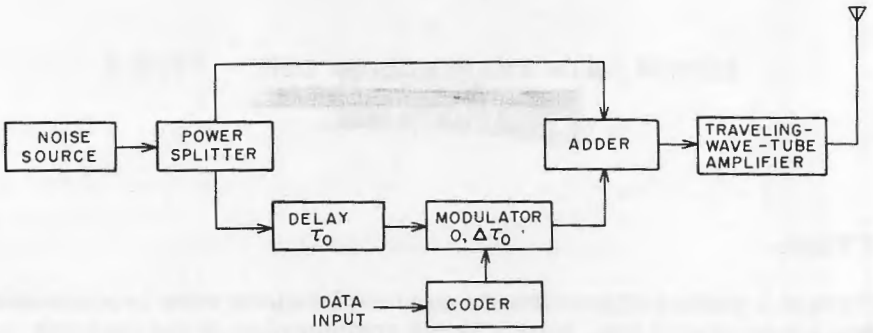

Fig. 1 - Block diagram of transmitter

To simplify the receiver further, the delay is inserted after the video amplifier (Fig. 2). This eliminates bulky cable, with its associated loss, from the r-f section and eliminates the need for dual mixers and video i-f amplifiers; however, restrictions are placed upon the frequency of the local oscillator.

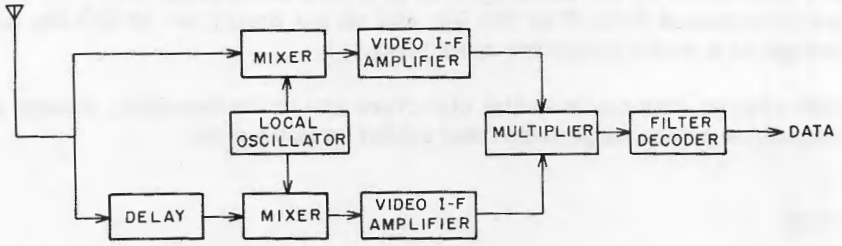

(a) r-f delay receiver

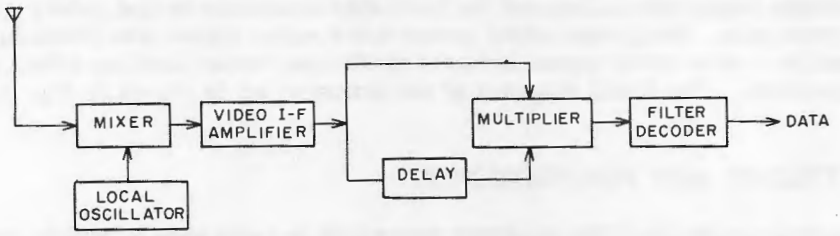

(b) Video i-f delay receiver

Fig. 2 - Basic block diagrams of DEMON receivers

The local oscillator is adjusted to a frequency such that

$$f_{L.O.} = n\left(\frac{1}{2\tau_o}\right), \tag{1}$$

where τ_o is the system delay and n is the integer giving the nearest frequency to the center of the r-f spectrum. This converts the transmitted r-f power spectrums to i-f power spectrums of the following form:

$$P_1(\omega) = [1 + \cos \omega\tau_o] \tag{2}$$

$$P_2(\omega) = [1 - \cos \omega(\tau_o + \Delta\tau_o)] \tag{3}$$

for

$$0 < \omega < \omega_n,$$

where ω_n is the i-f cutoff frequency or one-half the r-f bandwidth, and $\Delta\tau_o$ is the modulating delay time.

To examine the effects of the video i-f delay we take the auto-correlation functions of the resulting power spectrums:

$$\varphi_1(\tau) = \int_o^{\omega_n} P_1(\omega) \cos \omega\tau \, d\omega, \tag{4}$$

$$\varphi_2(\tau) = \int_o^{\omega_n} P_2(\omega) \cos \omega\tau \, d\omega, \tag{5}$$

which give

$$\varphi_1(\tau) = \frac{1}{\tau} \sin \omega_n\tau + \frac{\sin \omega_n(\tau_o - \tau)}{2(\tau_o - \tau)} + \frac{\sin \omega_n(\tau_o + \tau)}{2(\tau_o + \tau)}, \tag{6}$$

$$\varphi_2(\tau) = \frac{\sin \omega_n\tau}{\tau} - \frac{\sin \omega_n(\tau_o + \Delta\tau_o - \tau)}{2(\tau_o + \Delta\tau_o - \tau)} - \frac{\sin \omega_n(\tau_o + \Delta\tau_o + \tau)}{2(\tau_o + \Delta\tau_o + \tau)}, \tag{7}$$

where τ is the video i-f delay. These equations are plotted in Fig. 3 for $\omega_n = 2\pi \times 100$ Mc and $\tau_o = 20 \times 10^{-9}$ sec. By subtracting these two expressions,

$$\varphi_1(\tau) - \varphi_2(\tau) = \frac{\sin \omega_n(\tau_o - \tau)}{2(\tau_o - \tau)} + \frac{\sin \omega_n(\tau_o + \Delta\tau_o - \tau)}{2(\tau_o + \Delta\tau_o - \tau)} + \frac{\sin \omega_n(\tau_o + \tau)}{2(\tau_o + \tau)} + \frac{\sin \omega_n(\tau_o + \Delta\tau_o + \tau)}{2(\tau_o + \Delta\tau_o + \tau)}, \tag{8}$$

and plotting the magnitude of this function (Fig. 4), the resulting multiplier signal output voltage versus receiver delay is obtained. Compared with the r-f delay receiver in reference 1, the peak occurring at $\tau = \tau_o$ is broader and has no rapid fluctuations; however, detuning the local oscillator in the neighborhood of the proper frequency varies the multiplier output approximately as $|\cos 2\pi(\Delta f\tau_o)|$. Thus, varying the video i-f delay corresponds to a coarse adjustment of the delay in the r-f delay receiver and the tuning of the local oscillator to a vernier adjustment of the delay.

The signal-to-noise characteristic at the output of the multiplier, derived in Appendix A, and is shown to depend upon video i-f bandwidth, output bandwidth, and the effective signal-to-noise ratio in the r-f and i-f portions of the receiver. This relationship is

$$\left(\frac{S}{N}\right)_{out} \quad \frac{\alpha}{4\gamma}\left[\frac{1}{\left(\frac{N_r}{C} + 1\right)^2 + \frac{1}{2}}\right], \tag{9}$$

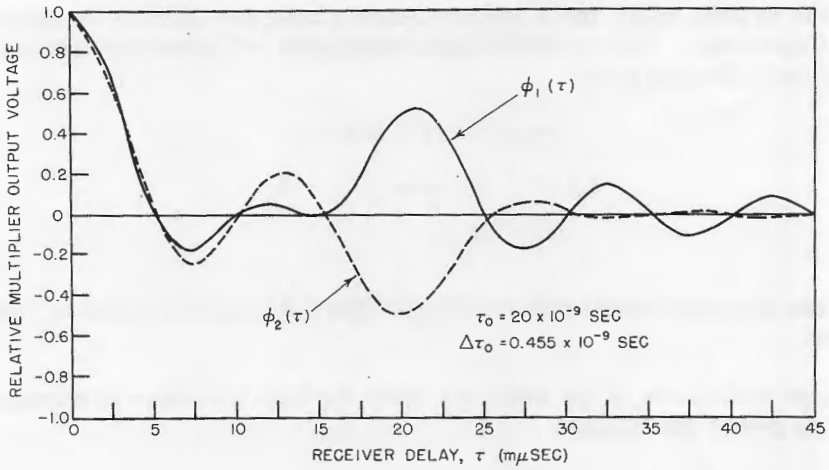

Fig. 3 - Multiplier response to i-f spectrums

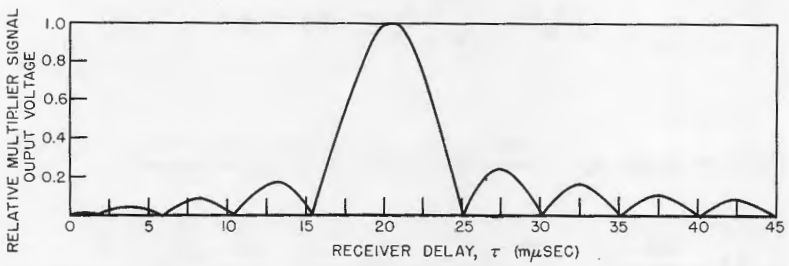

Fig. 4 - Multiplier signal output voltage vs. receiver delay

where

α = video i-f bandwidth,

γ = multiplier output bandwidth,

S = multiplier output signal power,

N = multiplier output noise power,

N_r = total receiver noise (external + internal) referred to input, and

C = input signal power.

This equation is plotted in Fig. 5 with experimentally determined data, using the bandwidth constants of α = 100 Mc and γ = 20 kc. The experimental curve is felt to approximate the theoretical curve; the discrepancy is believed to be due to the fact that ideal filters and rectangular noise spectrums are not attained in practice. A definite output signal-to-noise ratio is obtained even with zero or extremely low receiver noise, because the finite integration time of the receiver passes noise components of the carrier through the multiplier output bandwidth.

The intelligence in the multiplier output is in the form of a 75 kc signal which is frequency modulated with 300 to 3000 cycles of audio information. The output signal-to-noise ratio of the fm decoder for input signal-to-noise ratios greater than 6 db is (2)

$$r_o = \frac{\sqrt{3d}\, r_i(r_i^2 + 1)\gamma_c^{-1/2}}{[6d^2 + \gamma_c^2(r_i^2 + 1)^2]^{1/2}}, \quad (10)$$

where

r_o = output voltage signal-to-noise ratio

r_i = input voltage signal-to-noise ratio

$d = \frac{\text{frequency deviation}}{\text{half i-f bandwidth}} = \frac{3 \text{ kc}}{10 \text{ kc}} = 0.3$

$\gamma_c = \frac{\text{audio bandwidth}}{\text{half i-f bandwidth}} = \frac{3 \text{ kc}}{10 \text{ kc}} = 0.3.$

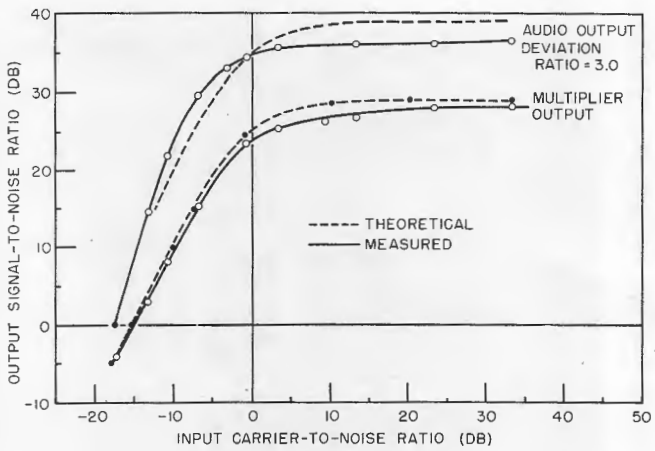

Fig. 5 - Signal-to-noise relationships in receiver (α = 100 Mc, γ = 20 kc)

The results of the above equation, with Eq. (9) as the input, are plotted in Fig. 5 with experimentally determined data.

RECEIVER INSTRUMENTATION

The video delay receiver for the DEMON data transmission system is shown in Figs. 6 and 7. Two ATR type racks were used to house the receiver, one containing the r-f, i-f, and multiplier circuitry and the other containing the subcarrier f-m decoder and power supply. A detailed block diagram is shown in Fig. 8.

The r-f portion of the receiver consists of a broadband r-f amplifier, mixer, and local oscillator. A type 416B microwave triode is used in a grounded grid circuit for the r-f amplifier because of its excellent transit-time conductance, high transconductance, and low interelectrode capacities (3). A balanced hybrid ring mixer (Fig. 9) using the

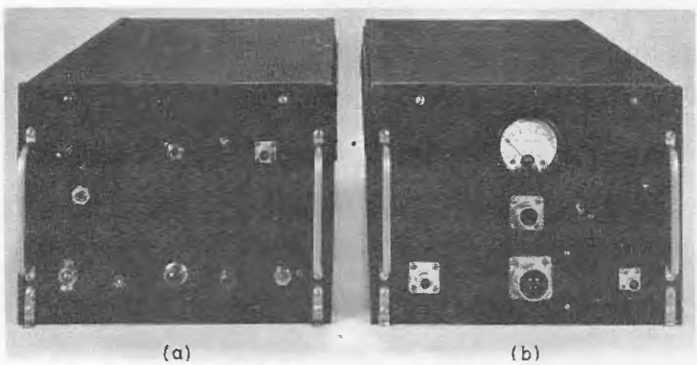

Fig. 6 - DEMON receiver. (a) Power supply and decoder unit; (b) r-f, i-f, and multiplier unit.

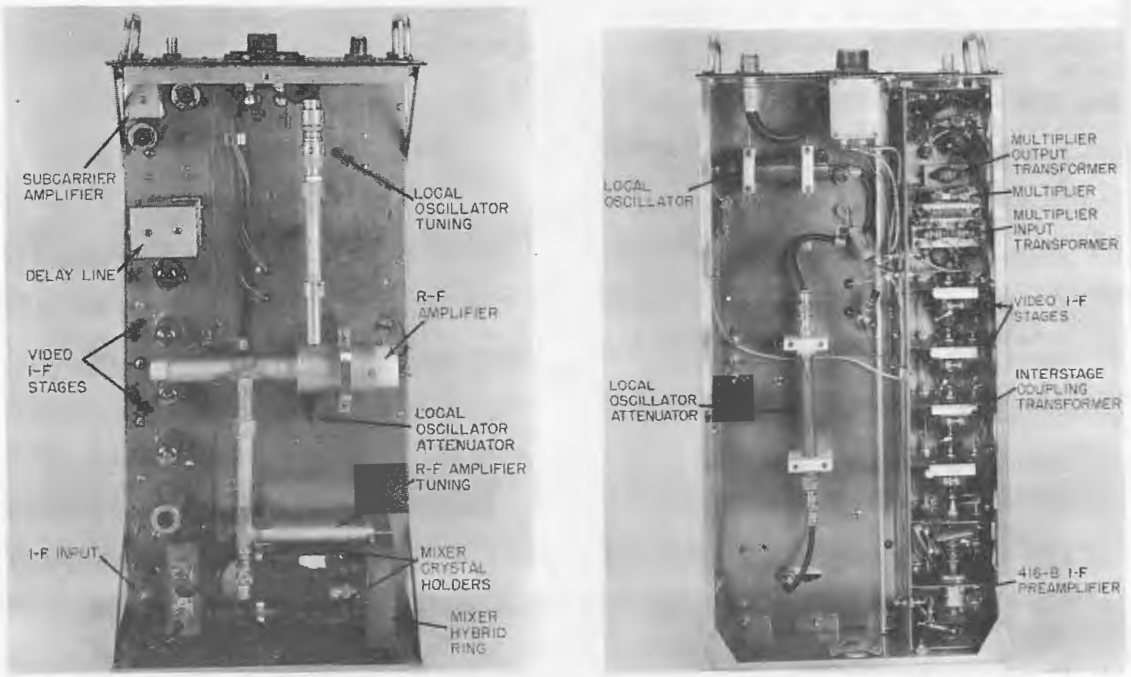

(a) Top view (b) Bottom view

Fig. 7 - R-f, i-f, and multiplier unit

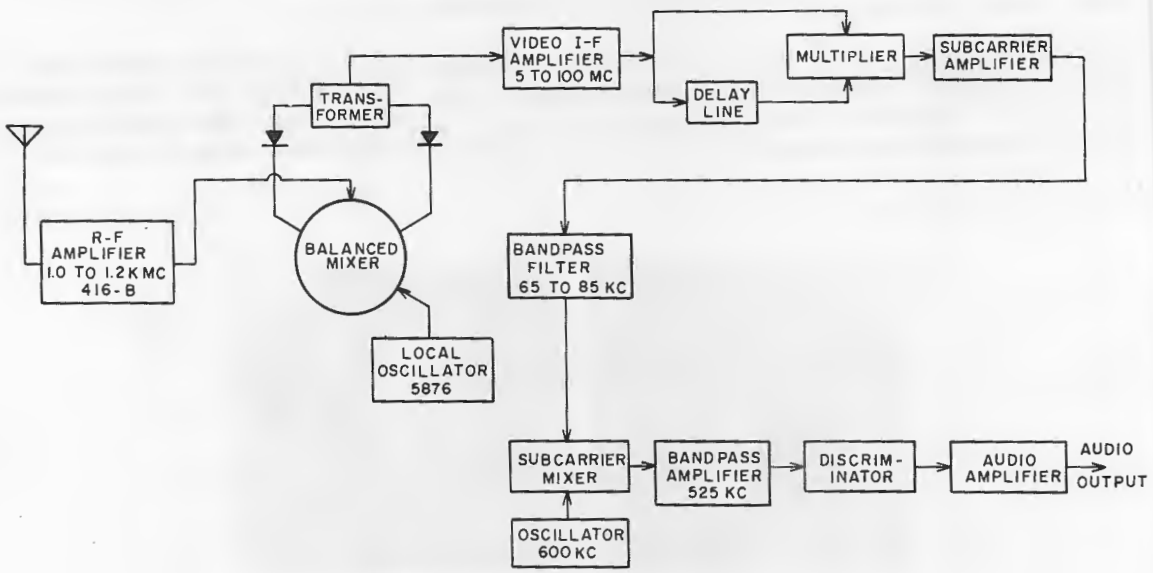

Fig. 8 - Detailed block diagram of receiver

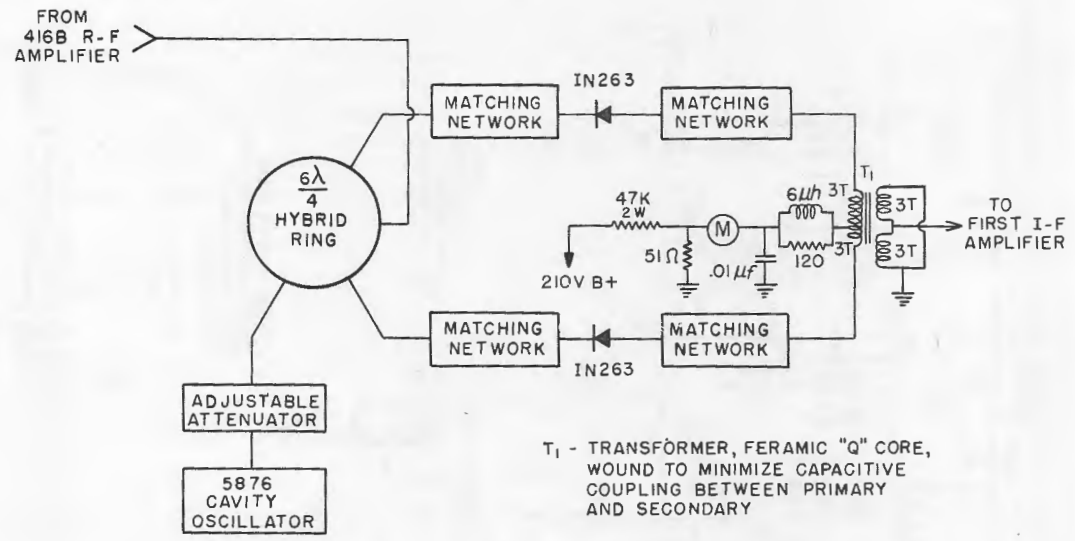

Fig. 9 - Basic diagram of r-f mixer

newly developed 1N263 germanium microwave diodes proved to be slightly superior to mixers using silicon diodes. Wideband coupling with low loss is accomplished between the mixer and i-f by the use of a rectangular ferrite-core transformer whose coupling coefficient is very nearly unity. The small leakage reactance is tuned in the network to support the high end of the i-f spectrum, while the lower frequency cutoff is determined by the primary inductance of the transformer and output impedance of the mixer. The local oscillator is a small cavity-resonated type 5675 pencil triode with a capacity-probe vernier tuning adjustment.

The video i-f portion of the receiver consists of one 416-B, one 6BQ7-A, and four 5857 stages of amplification (Fig. 10). The type 416-B triode operated successfully at low frequencies, although it was originally designed for use at microwave frequencies. This tube provides a voltage gain of six and a noise figure of approximately 3.0 db in this particular circuitry. A noise figure in the neighborhood of 1.2 db theoretically may be obtained with this tube by increasing the driving impedance; however, the resulting loss in gain makes this impractical. The 6BQ7-A stage of amplification is used to provide enough signal to overcome the noise that seems to be inherent in the type 5857 secondary-emission tubes. The 5857 tubes have a transconductance of 20,000 microhms and moderate interelectrode capacities with only 2.6 milliamperes of cathode current, thus providing excellent gain and low power consumption; however, the critical nature of the electrode potentials require a well regulated power supply.

Interstage coupling networks are of the four-terminal type utilizing constant K and terminating half-section filters as described in reference 4. To match the input and output capacities of the tubes properly, ferrite transformers with nearly unity coupling are inserted in the interstage networks. By careful winding, the leakage inductance is kept low enough so that it may be absorbed into the filter structure, and the primary inductance is kept large enough to provide the desired low-frequency response. A slight amount of peaking is designed into the networks in the neighborhood of 100 Mc to compensate for input transit-time loading of the vacuum tubes. The combined frequency response of the r-f and i-f sections of the receiver, and the response of the i-f above are plotted in Figs. 11 and 12. A broadband fluorescent-tube noise source was used to measure the receiver noise figure, which was found to be 11 db.

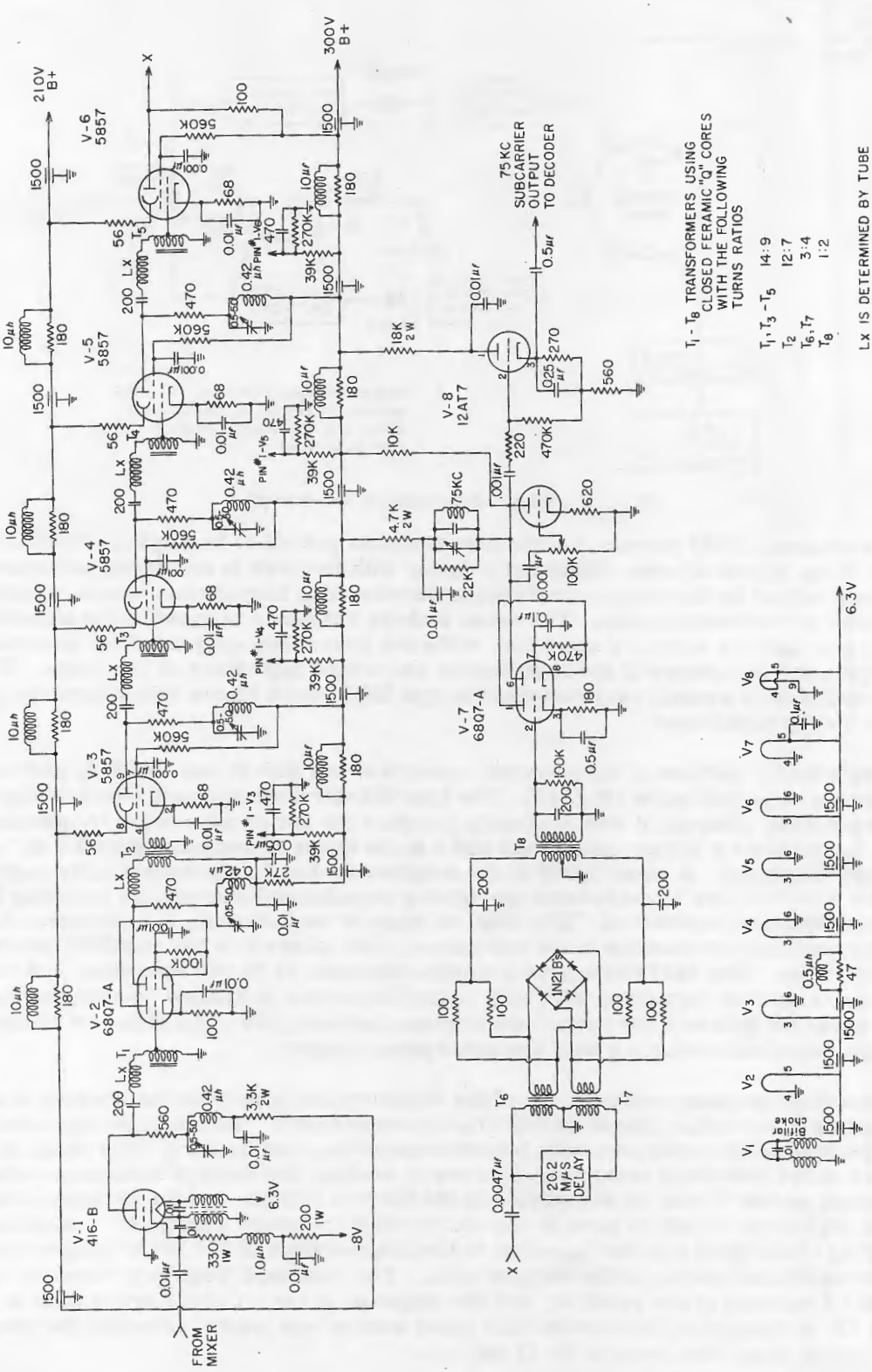

Fig. 10 - Diagram of i-f and multiplier circuits

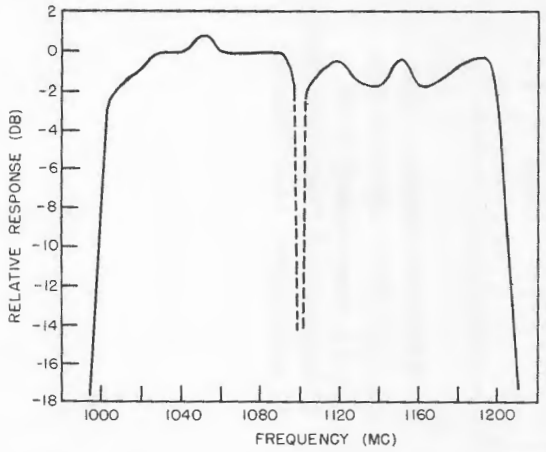

Fig. 11 - Frequency response of receiver

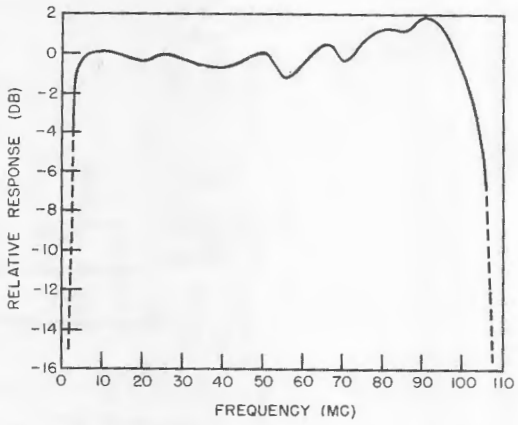

Fig. 12 - Frequency response of video i-f amplifier

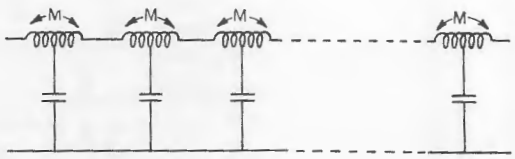

Fig. 13 - Video i-f delay

The video i-f delay is constructed in a small plug-in unit to facilitate changing when required. This delay is of the low-pass filter type using negative mutual coupling between the inductive elements (Fig. 13). From reference 5, a filter design factor of m = 1.34, a characteristic impedance of 100 ohms and a cutoff frequency of 160 Mc were selected to provide a delay of 2.53 millimicroseconds per filter section. For the experimental tests of this report, eight filter sections are used to obtain a delay of 20.2 millimicroseconds.

A diode ring multiplier composed of 1N21B silicon diodes is used as the correlation detector. In reference 6 it is shown that under small-signal conditions the diode characteristics become square law, thus making this circuit a good low-level multiplier. This is particularly desirable in this equipment, because it requires less amplification in the wideband video i-f stages. The output of the multiplier is the frequency-modulated 75 kc subcarrier, which is amplified before being fed to the subcarrier decoder.

The subcarrier decoder is located on the chassis with the receiver power supply. A bandpass filter, 65 kc to 85 kc, is located at the input to the mixer tube of the decoder to remove any undesirable system noise. The decoder is basically a superheterodyne fm receiver as shown in the block diagram in Fig. 8. A local oscillator frequency of 600 kc is used to provide a difference frequency of 525 kc for the i-f stages. The filter network in the cathode of the first i-f stage provides increased rejection of the local oscillator signal, while the other circuitry is conventional. Schematic diagrams of the decoder and receiver power supply are shown in Figs. 14 and 15.

PROPAGATION CHARACTERISTICS

Preliminary analysis of the DEMON data transmission system indicates that it should be superior to conventional narrow-band data transmission systems, in which fading at the receiving antenna is caused by the interaction of two or more propagation

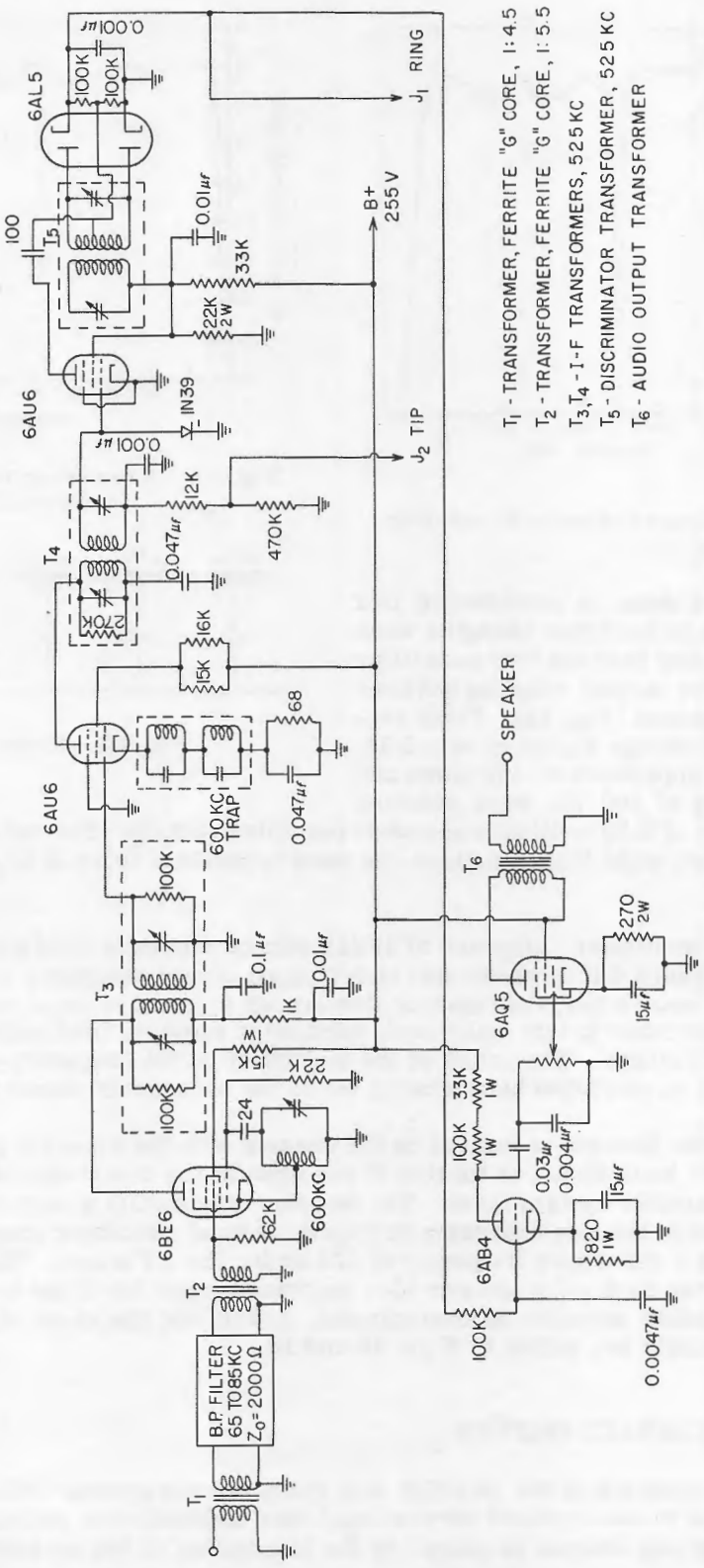

Fig. 14 - Circuit diagram of sub-carrier decoder

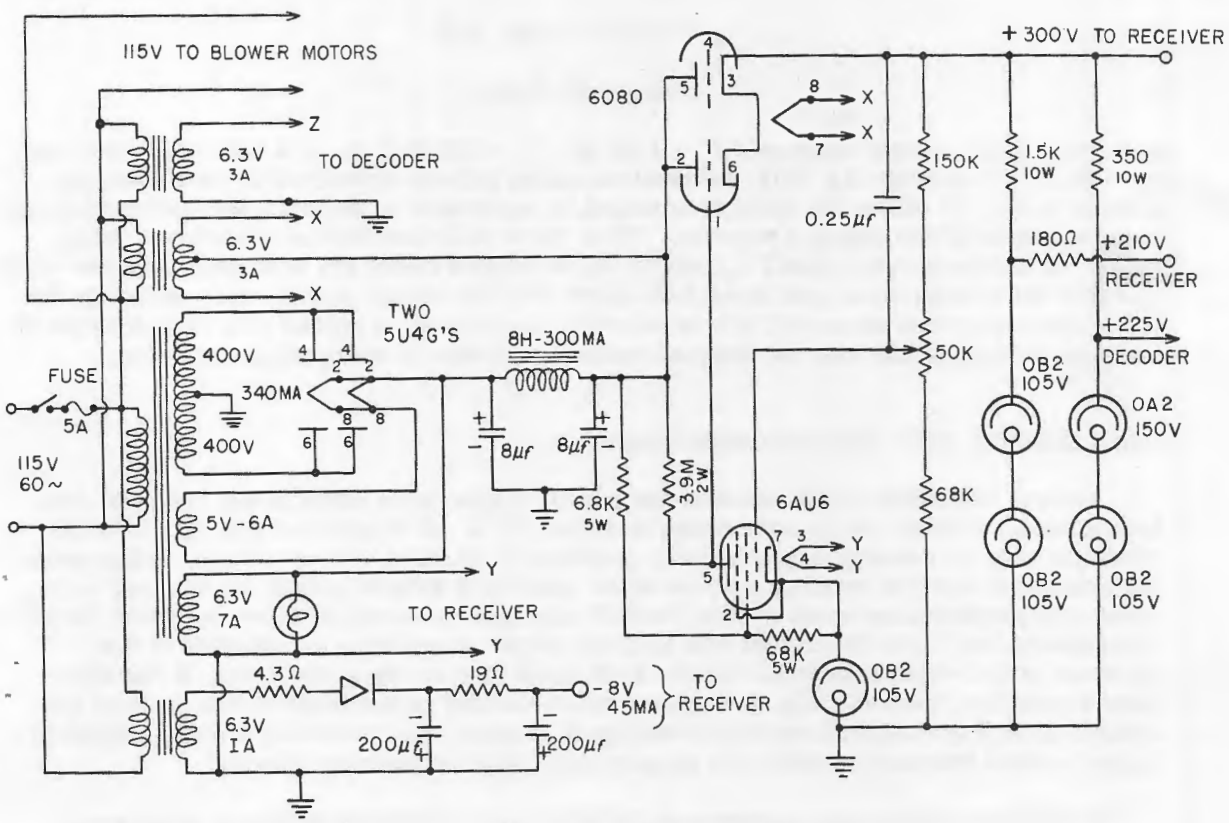

Fig. 15 - Circuit diagram of receiver power supply

paths between the transmitter and receiver. This indicates that a system of this type should be adaptable to scatter links, or to transmission over sea water where multipath fading can be a serious problem.

Assuming the extreme case in which propagation takes place over a perfect reflector and isotropic antennas are used, we obtain from Appendix B

$$E_{(\tau_1)} = 1 + \cos \omega_o \tau_1 \left\{ \frac{\sin \omega_b \tau_1}{2\omega_b} \left[-\frac{1}{\tau_1} - \frac{1}{2(\tau_1 + 2\tau_o)} + \frac{1}{2(2\tau_o - \tau_1)} \right] \right.$$

$$+ \frac{\sin \omega_b (\tau_1 + \Delta\tau_o)}{4\omega_b} \left[-\frac{1}{\tau_1 + \Delta\tau_o} - \frac{1}{2\tau_o + \tau_1 + \Delta\tau_o} \right]$$

$$\left. + \frac{\sin \omega_b (\tau_1 - \Delta\tau_o)}{4\omega_b} \left[-\frac{1}{\tau_1 - \Delta\tau_o} + \frac{1}{2\tau_o - \tau_1 + \Delta\tau_o} \right] \right\}, \qquad (11)$$

where

$E_{(\tau_1)}$ = relative multiplier output voltage,

$f_o = \frac{\omega_o}{2\pi}$ = center frequency of spectrum,

$f_b = \frac{\omega_b}{2\pi}$ = bandwidth of spectrum,

τ_o = system delay, and

τ_1 = multipath delay.

Substituting the system constants f_o = 1100 Mc, f_b = 200 Mc, $\Delta\tau_o = 0.445 \times 10^{-9}$ sec, and $\tau_o = 20 \times 10^{-9}$ sec into Eq. (11), the relative fading pattern compared to free space is plotted in Fig. 16 where the multiplier output is expressed in decibels and multipath delay in wavelengths of the center frequency. This curve indicates that no significant fades occur for delays greater than 3 λ_o, except in the region where the multipath delay is equal to twice the system delay and fades 6 db below average signal level occur. Although the ideal case described above will not be obtained in practice, it should give an indication of the type of results that may be obtained under conditions of multipath propagation.

CONCLUSIONS AND RECOMMENDATIONS

Several important improvements and modifications were made in the DEMON data transmission system, as recommended in reference 1. It is believed that the DEMON principle may now be applied in several operational situations to advantage. It has been demonstrated that the receiver may be made small and simple enough for tactical employment with performance equal to that theoretically predicted within a few decibels. It has been determined from bench test that a usable output signal may be obtained at the receiver output with as little as minus 13-db input carrier-to-noise ratio. It has also been shown that, theoretically, a wideband noisy carrier is excellent coding against the effects of such propagation noises as multipath, scatter, and receiving antenna shielding (experimental propagation data will be presented in a forthcoming report).

A study into the tactical aspects of DEMON data transmission link is being made, and when the results of this study are reported, recommendations will be made on possible equipment configuration for various tasks (i.e., propagation noise reduction, secure tactical data transmission). It appears at present that the above areas are the only ones in which a justification may be made for the large bandwidth requirements of DEMON systems.

ACKNOWLEDGMENTS

The authors wish to extend their thanks to Mr. Stanley D. Fawley and Mr. Richard B. McWhirt who constructed and tested most of the equipment.

* * *

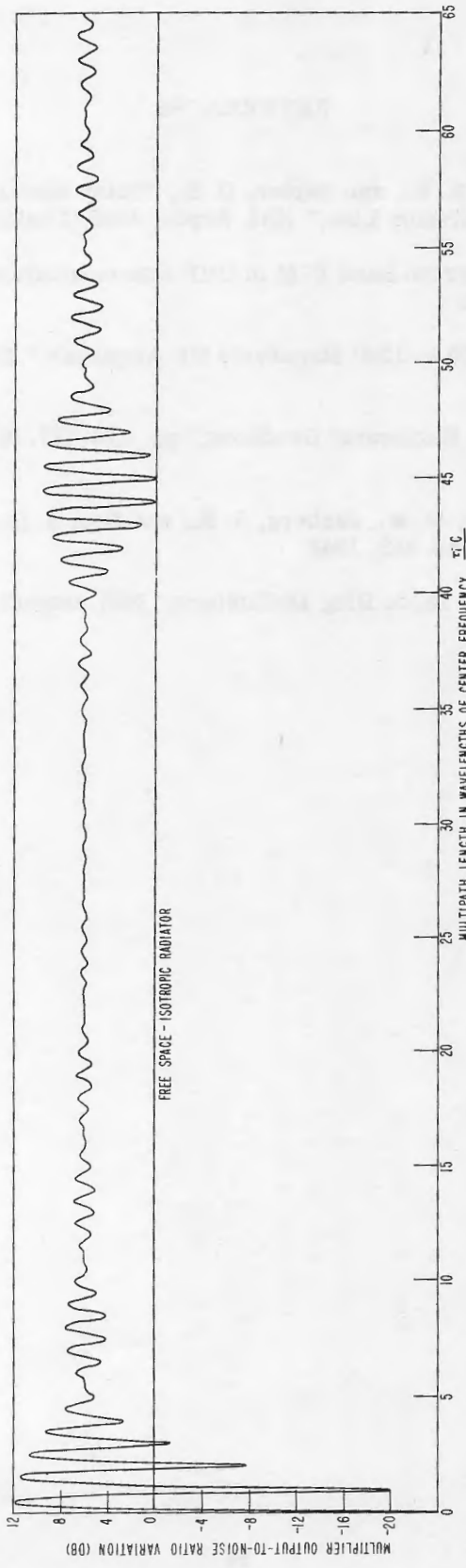

Fig. 16 - Multipath propagation characteristics

[redacted]

REFERENCES

1. Brodzinsky, A., Zirm, R. R., and Hepler, D. S., "Delay Modulated Noise Carrier (DEMON) Data Transmission Link," NRL Report 4390 (Confidential), 27 August 1954

2. Toth, E., "A-M and Narrow-Band F-M in UHF Communications (Part II)," Electronics 22:102-108, March 1949

3. McWhirt, R. B., "A 1000 to 1200 Megacycle RF Amplifier," NRL Report 4470, 5 January 1955

4. Terman, F. E., "Radio Engineers' Handbook," pp. 413-427, New York: McGraw-Hill, 1943

5. Ginzton, E. L., Hewlett, W. R., Jasberg, J. H., and Noe, J. D., "Distributed Amplification," Proc. I.R.E. 36:956-969, 1948

6. Wilcox, R. H., "Crystal Diode Ring Multipliers," NRL Report 4385, June 18, 1954

[redacted]

APPENDIX A
Computation of Signal-to-Noise Characteristics at Output of Multiplier

The video i-f portion of the receiver described in the body of this report contains a spectrum of noise (Fig. A1) resulting from ambient receiver noise (external + internal) and a spectrum of received signal noise.

Let ω_α be the video i-f cutoff frequency, N_r the ambient receiver noise power, and $p(\omega)$ the ambient noise spectrum:

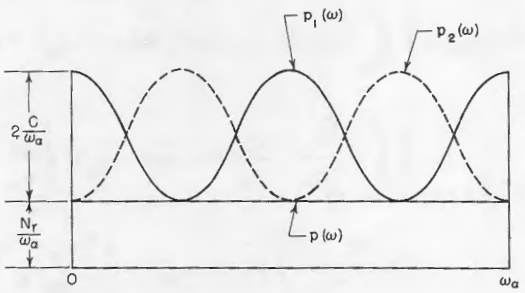

Fig. A1 - Spectrums of i-f noise

$$p(\omega) = \frac{N_r}{\omega_\alpha} \text{ for } 0 < \omega < \omega_\alpha, \qquad (A1)$$
$$= 0 \text{ for all other } \omega.$$

Let C be the average received signal power, τ_o the system delay, and $\Delta\tau_o$ the system modulating delay. Then $p_1(\omega)$ and $p_2(\omega)$ will be the two received signal power spectra converted to video i-f frequencies, which are received alternately on an average equal time basis:

$$\left.\begin{aligned} p_1(\omega) &= \frac{C}{\omega_\alpha}[1 + \cos \omega\tau_o] && \text{for } 0 < \omega < \omega_\alpha, \\ &= 0 && \text{for all other } \omega; \end{aligned}\right\} \qquad (A2)$$

$$\left.\begin{aligned} p_2(\omega) &= \frac{C}{\omega_\alpha}[1 - \cos \omega(\tau_o + \Delta\tau_o)] && \text{for } 0 < \omega < \omega_\alpha, \\ &= 0 && \text{for all other } \omega. \end{aligned}\right\} \qquad (A3)$$

If $\overline{V}_1$, and $\overline{V}_2$ are the multiplier output voltages resulting from the product of the split, delayed, and multiplied video i-f spectrums, then $(\overline{V}_1 - \overline{V}_2)$ will be the peak-to-peak signal voltage output of the multiplier. Now,

$$\overline{V}_1 = \varphi_1(\tau_o) = \int_o^{\omega_\alpha} [p(\omega) + p_1(\omega)] \cos \omega\tau_o \, d\omega,$$

and

$$\overline{V}_2 = \varphi_2(\tau_o) = \int_o^{\omega_\alpha} [p(\omega) + p_2(\omega)] \cos \omega\tau_o \, d\omega.$$

Therefore

$$\overline{V_1 - V_2} = \int_o^{\omega_\alpha} [p_1(\omega) - p_2(\omega)] \cos \omega\tau_o \, d\omega = \frac{C}{\omega_\alpha}\int_o^{\omega_\alpha} [\cos \omega\tau_o + \cos \omega(\tau_o + \Delta\tau_o)] \cos \omega\tau_o \, d\omega$$

$$= C\left[\frac{1}{2} + \frac{\sin \omega_\alpha\Delta\tau_o}{2\omega_\alpha\Delta\tau_o} + \frac{\sin \omega_\alpha(2\tau_o)}{4\omega_\alpha\tau_o} + \frac{\sin \omega_\alpha(2\tau_o + \Delta\tau_o)}{2\omega_\alpha(2\tau_o + \Delta\tau_o)}\right]. \qquad (A4)$$

The noise spectrum on the output of the multiplier for frequencies in the region where $\omega_m \ll \omega_\alpha$ may be very nearly approximated by calculating the difference-frequency components resulting from the multiplying action, where ω_m is the multiplier output frequency after other components are removed by filtering. The output power spectrums for $\omega_m \ll \omega_\alpha$ are defined as $P_1(\omega_m)$ and $P_2(\omega_m)$:

$$P_1(\omega_m) = \frac{1}{2}\int_{\omega_m}^{\omega_\alpha} [p(\omega) + p_1(\omega)]\,[p(\omega - \omega_m) + p_1(\omega - \omega_m)]\; d\omega$$

$$= \frac{1}{2}\int_{\omega_m}^{\omega_\alpha} \left[\frac{N_r}{\omega_\alpha} + \frac{C}{\omega_\alpha}(1 + \cos\,\omega\tau_o)\right]\left\{\frac{N_r}{\omega_\alpha} + \frac{C}{\omega_\alpha}[1 + \cos(\omega - \omega_m)\tau_o]\right\} d\omega$$

$$= \frac{1}{2}\left\{\left(\frac{N_r + C}{\omega_\alpha}\right)^2 (\omega_\alpha - \omega_m) + \frac{C^2(\omega_\alpha - \omega_m)}{2\omega_\alpha{}^2} \cos\,\omega_m\tau_o + \frac{C(N_r + C)}{\omega_\alpha{}^2\tau_o}(\sin\,\omega_\alpha\tau_o - \sin\,\omega_m\tau_o)\right.$$

$$\left. + \frac{C(N_r + C)}{\omega_\alpha{}^2\tau_o} \sin\,(\omega_\alpha - \omega_m)\tau_o + \frac{C^2}{4\omega_\alpha{}^2\tau_o}[\sin\,(2\omega_\alpha - \omega_m)\tau_o - \sin\,\omega_m\tau_o]\right\}.$$

For the case where $\omega_\alpha \gg \omega_m$ and $\omega_m\tau_o$ is extremely small,

$$P_1(\omega_m) = \frac{1}{2}\left\{\frac{(N_r + C)^2}{\omega_\alpha} + \frac{C^2}{2\omega_\alpha} + \frac{2C(N_r + C)}{\omega_\alpha{}^2\tau_o} \sin\,\omega_\alpha\tau_o + \frac{C^2}{4\omega_\alpha{}^2\tau_o} \sin\,2\omega_\alpha\tau_o\right\}.$$

In like manner

$$P_2(\omega_m) = \frac{1}{2}\left\{\frac{(N_r + C)^2}{\omega_\alpha} + \frac{C^2}{2\omega_\alpha} - \frac{2C(N_r + C)}{\omega_\alpha{}^2(\tau_o + \Delta\tau_o)} \sin\,\omega_\alpha(\tau_o + \Delta\tau_o) + \frac{C^2}{4\omega_\alpha{}^2(\tau_o + \Delta\tau_o)} \sin\,2\omega_\alpha(\tau_o + \Delta\tau_o)\right\}.$$

Taking the average value of the two spectrums (because they are received alternately) gives

$$P(\omega_m) = \frac{1}{2}[P_1(\omega_m) + P_2(\omega_m)]$$

$$= \frac{N_r{}^2 + 2N_rC + \frac{3}{2}C^2}{2\omega_\alpha} + \frac{C(N_r + C)}{2\omega_\alpha{}^2\tau_o} \sin\,\omega_\alpha\tau_o - \frac{C(N_r + C)}{2\omega_\alpha{}^2(\tau_o + \Delta\tau_o)} \sin\,\omega_\alpha(\tau_o + \Delta\tau_o)$$

$$+ \frac{C^2}{16\,\omega_\alpha{}^2\tau_o} \sin\,2\omega_\alpha\tau_o + \frac{C^2}{16\,\omega_\alpha{}^2(\tau_o + \Delta\tau_o)} \sin\,2\omega_\alpha(\tau_o + \Delta\tau_o). \qquad \text{(A5)}$$

If a bandpass filter is placed on the output with cutoff frequencies ω_1 and ω_2 to pass the information, the output noise is

$$N = \int_{\omega_1}^{\omega_2} P(\omega_m)\; d\omega_m. \qquad \text{(A6)}$$

With the output filter cutoff frequencies ω_1, and ω_2, the fundamental frequency of the information is passed. Then from Eq. (A4) the output signal power is

$$S = \frac{(V_1 - V_2)^2}{8}, \tag{A7}$$

or the output signal-to-noise ratio becomes

$$\left(\frac{S}{N}\right)_{out} = \frac{\frac{(V_1 - V_2)^2}{8}}{\int_{\omega_1}^{\omega_2} P(\omega_m)\, d\omega_m}. \tag{A8}$$

To find a simple solution for system values used in the body of this report, the following values are used:

$$\tau_o = 20 \times 10^{-9} \text{ sec},$$

$$\omega_\alpha = 2\pi \times 100 \text{ Mc},$$

$$\omega_1 = 2\pi \times 65 \text{ kc},$$

$$\omega_2 = 2\pi \times 85 \text{ kc}.$$

Now define

$$\omega_\gamma = 2\pi\gamma = \omega_2 - \omega_1 = 2\pi \times 20 \text{ kc}$$

and

$$\omega_\alpha = 2\pi\alpha.$$

Then

$$S = \frac{C^2}{8} \tag{A9}$$

and

$$N = \frac{\gamma\,(N_r^2 + 2N_rC + \frac{3}{2}C^2)}{2\alpha}. \tag{A10}$$

From Eqs. (A1), (A2), and (A3), the average video i-f signal noise power and receiver noise power are respectively C and N_r. This may be used to define the video i-f signal-to-noise ratio as C/N_r. The output signal-to-noise ratio is then very closely approximated by

$$\left(\frac{S}{N}\right)_{out} = \frac{\alpha}{4\gamma}\left[\frac{1}{\left(\frac{N_r}{C} + 1\right)^2 + \frac{1}{2}}\right], \tag{A11}$$

where

α = video i-f bandwidth,

γ = multiplier output bandwidth, and

$\frac{C}{N_r}$ = video i-f signal-to-noise ratio.

Substituting $\alpha = 100$ Mc and $\gamma = 20$ kc,

$$\left(\frac{S}{N}\right)_{out} = \frac{1250}{\left(\frac{N_r}{C} + 1\right)^2 + \frac{1}{2}}. \qquad \text{(A12)}$$

APPENDIX B
Computation of Multiplier Output Signal Fading Under Multipath Propagation Conditions

This analysis will demonstrate the effect of fading with respect to free space propagation where there are two paths of propagation between transmitting and receiving antennas. This may be a direct path and a path resulting from perfect reflection from an external object such as water. The conditions of 180° phase shift on reflection and the power in each path equal will also be assumed.

The two transmitted spectrums are of the following form:

$$\left.\begin{aligned} P_1'(\omega) &= \frac{P}{2\omega_b}(1 + \cos\ \omega\tau_o) && \text{for } \omega_m < \omega < \omega_n, \\ &= 0 && \text{for all other } \omega; \end{aligned}\right\} \quad \text{(B1)}$$

$$\left.\begin{aligned} P_2'(\omega) &= \frac{P}{2\omega_b}[1 + \cos\ \omega(\tau_o + \Delta\tau_o)] && \text{for } \omega_m < \omega < \omega_n, \\ &= 0 && \text{for all other } \omega. \end{aligned}\right\} \quad \text{(B2)}$$

After being propagated over two paths, the received power spectrums are equivalent to what would be obtained by passing the spectrum received through free space conditions through a filter having a response of $2(1 - \cos\ \omega\tau_1)$. Thus the received power spectrums become

$$\left.\begin{aligned} P_1(\omega) &= \frac{P}{\omega_b}[1 + \cos\ \omega\tau_o][1 - \cos\ \omega\tau_1] && \text{for } \omega_m < \omega < \omega_n, \\ &= 0 && \text{for all other } \omega; \end{aligned}\right\} \quad \text{(B3)}$$

and

$$\left.\begin{aligned} P_2(\omega) &= \frac{P}{\omega_b}[1 + \cos\ \omega(\tau_o + \Delta\tau_o)][1 - \cos\ \omega\tau_1] && \text{for } \omega_m < \omega < \omega_n, \\ &= 0 && \text{for all other } \omega, \end{aligned}\right\} \quad \text{(B4)}$$

where

$\frac{\omega_m}{2\pi}$ = lower cutoff frequency of transmitted spectrum,

$\frac{\omega_n}{2\pi}$ = upper cutoff frequency of transmitted spectrum,

τ_o = receiver and transmitter delay,

$\Delta\tau_o$ = transmitter modulating delay,

τ_1 = difference in delay between paths, and

$\beta = \frac{\omega_b}{2\pi} = \frac{\omega_n - \omega_m}{2(2\pi)}$ = half r-f bandwidth.

Let $\bar{V}_1$ and $\bar{V}_2$ be the multiplier output voltages for the received spectrums and $(\bar{V}_1 - \bar{V}_2)$ the peak-to-peak signal voltage out of the multiplier:

$$\bar{V}_1 = \frac{P}{\omega_b} \int_{\omega_m}^{\omega_n} P_1(\omega) \cos \omega\tau_o \, d\omega$$

and

$$\bar{V}_2 = \frac{P}{\omega_b} \int_{\omega_m}^{\omega_n} P_2(\omega) \cos \omega\tau_o \, d\omega.$$

Then

$$\bar{V}_1 - \bar{V}_2 = \frac{P}{\omega_b} \int_{\omega_m}^{\omega_n} [P_1(\omega) - P_2(\omega)] \cos \omega\tau_o \, d\omega$$

$$= \frac{P}{\omega_b} \int_{\omega_m}^{\omega_n} [\cos \omega\tau_o - \cos \omega(\tau_o + \Delta\tau_o) - \cos \omega\tau_o \cos \omega\tau_1 + \cos \omega(\tau_o + \Delta\tau_o) \cos \omega\tau_1] \cos \omega\tau_o \, d\omega. \quad \text{(B5)}$$

The center frequency of the r-f spectrum is defined as

$$f_o = \frac{\omega_o}{2\pi} = \frac{\omega_n + \omega_m}{2(2\pi)}.$$

The variation of the multiplier output voltage with respect to τ_1 is

$$V_o = \frac{V_1 - V_2}{P} = 2\left[\frac{1}{2} - \frac{\sin \omega_b\Delta\tau_o \cos \omega_o\Delta\tau_o}{2\omega_b\Delta\tau_o} + \frac{\sin \omega_b(2\tau_o) \cos \omega_o(2\tau_o)}{4\omega_b\tau_o}\right.$$

$$- \frac{\sin \omega_b(2\tau_o + \Delta\tau_o) \cos \omega_o(2\tau_o + \Delta\tau_o)}{2\omega_b(2\tau_o + \Delta\tau_o)} - \frac{\sin \omega_b\tau_1 \cos \omega_o\tau_1}{2\omega_b\tau_1}$$

$$+ \frac{\sin \omega_b(\tau_1 + \Delta\tau_o) \cos \omega_o(\tau_1 + \Delta\tau_o)}{4\omega_b(\tau_1 + \Delta\tau_o)} + \frac{\sin \omega_b(\tau_1 - \Delta\tau_o) \cos \omega_o(\tau_1 - \Delta\tau_o)}{4\omega_b(\tau_1 - \Delta\tau_o)}$$

$$- \frac{\sin \omega_b(\tau_1 + 2\tau_o) \cos \omega_o(\tau_1 + 2\tau_o)}{4\omega_b(\tau_1 + 2\tau_o)} - \frac{\sin \omega_b(2\tau_o - \tau_1) \cos \omega_o(2\tau_o - \tau_1)}{4\omega_b(2\tau_o - \tau_1)}$$

$$+ \frac{\sin \omega_b(2\tau_o + \tau_1 + \Delta\tau_o) \cos \omega_o(2\tau_o + \tau_1 + \Delta\tau_o)}{4\omega_b(2\tau_o + \tau_1 + \Delta\tau_o)}$$

$$\left. + \frac{\sin \omega_b(2\tau_o - \tau_1 + \Delta\tau_o) \cos \omega_o(2\tau_o - \tau_1 + \Delta\tau_o)}{4\omega_b(2\tau_o - \tau_1 + \Delta\tau_o)}\right]. \quad \text{(B6)}$$

From Eqs. (B1) and (B2), the multiplier output with one path of propagation is

$$V_o' = \frac{1}{P}\int_{\omega_m}^{\omega_n} [P_1'(\omega) - P_2'(\omega)] \cos \omega\tau_o \, d\omega$$

$$= \frac{1}{2} - \frac{\sin \omega_b(\Delta\tau_o) \cos \omega_o(\Delta\tau_o)}{2\omega_b\Delta\tau_o} + \frac{\sin \omega_b(2\tau_o) \cos \omega_o(2\tau_o)}{4\omega_b\tau_o}$$

$$- \frac{\sin \omega_b(2\tau_o + \Delta\tau_o) \cos \omega_o(2\tau_o + \Delta\tau_o)}{2\omega_b(2\tau_o + \Delta\tau_o)}. \qquad \text{(B7)}$$

If $E(\tau_1)$ is the multiplier output voltage variation with respect to one path of propagation or free space, from Eqs. (B6) and (B7)

$$E(\tau_1) = \frac{V_o}{V_o'}. \qquad \text{(B8)}$$

To find the special solution for system values used in the body of this report, the following values are used:

$$\tau_o = 20 \times 10^{-9} \text{ sec},$$

$$\Delta\tau_o = 0.455 \times 10^{-9} \text{ sec},$$

$$\omega_o = 2\pi \times 1100 \text{ Mc},$$

$$\omega_b = 2\pi \times 100 \text{ Mc}.$$

Substituting the above values in Eqs. (B6) and (B7) yields the following solution of $E(\tau_1)$ for the special case:

$$E(\tau_1) = 2 - 2 \cos \omega_o\tau_1 \left\{ \frac{\sin \omega_b\tau_1}{2\omega_b}\left[\frac{1}{\tau_1} + \frac{1}{2(\tau_1 + 2\tau_o)} - \frac{1}{2(2\tau_o - \tau_1)}\right] \right.$$

$$+ \frac{\sin \omega_b(\tau_1 + \Delta\tau_o)}{4\omega_b}\left[\frac{1}{(\tau_1 + \Delta\tau_o)} + \frac{1}{(2\tau_o + \tau_1 + \Delta\tau_o)}\right]$$

$$\left. + \frac{\sin \omega_b(\tau_1 - \Delta\tau_o)}{4\omega_b}\left[\frac{1}{(\tau_1 - \Delta\tau_o)} - \frac{1}{(2\tau_o - \tau_1 + \Delta\tau_o)}\right]\right\}.$$

NAVY-DPPO PRNC. WASH. D.C